

# Hopf Bifurcation of a hematopoietic regulation system

Suqi Ma<sup>1</sup>, Jinzhi Lei<sup>2</sup>

<sup>1</sup> Department of Mathematics, Chinese Agricultural University, Beijing 100083, China

<sup>2</sup>Zhou-Pei-Yuan Center for Applied Mathematics, Tsinghua University, Beijing 100083, China

## Abstract

A delay differential equations which to describe a generic two compartments blood cell model which originates from hematopoietic stem cell compartment to period neutrophil blood diseases is discussed. The kinetics of peripheral neutrophil and auto-regulation of hematopoietic stem cells are both supposed to be negative feedback mechanism and governed by Holling function. By applying geometrical criterion in analyzing stability of parameter region of steady states, we track the Hopf bifurcation position which is believed to give rise to blood cell oscillations in periodic neutropenia or other blood cell diseases.

**Keywords:** Hopf bifurcation; Hematopoietic regulation; Stem cells; Neutropenia.

## 1. Introduction

The interaction relationships between the mature stem cells and their peripheral tissues are of intention and increasing interest in biomedical sciences. To understand the interesting aspects of stem cells within

its tissue organization, the main feature of stem cells is illustrated. With the exception of the property of self-renewal and differentiation potential, stem cells own the ability to undergo cell divisions, exist in a mitotically quiescent state. Stem cells also can be functioned as the clonally regenerate cells of all the different cell types that consist the tissue in which they exist. Alike "erythropoiesis" model, oscillation arise in stem cell population is the consequence of the loss of stability of homeostasis state, which is dominated by auto-regulatory loops with negative feedback control mechanism[1-4].

Due to dysfunctions in regulatory control process of blood cell production, some hematological diseases emerge. Cyclical neutropenia(CN) has been the most extensively studied hematological disorder. Periodically, circulating neutrophil falls in the dynamic states with its count varying from normal counts to low levels[5,6,7]. The population of neutrophils, a type of granulocyte cell, is highest

among white blood cells in an ordinary level with 45 to 75 percent and low number abnormally.

The period of human with CN is typically reported to vary in the range of 19 to 21 days, and longer periods occur in some patients with 40 to 80 days[6,7]. It is now clear in grey collie that neutrophils oscillates from normal to extremely low levels suffering from a similar disease with the exception of the period ranging from 11 to 15 days. Therefore, people use the contrast experiment results of grey collie to discover CN oscillating character to human being. Mathematically, with link to blood cell production and negative feedback regulation mechanism, the cyclical neutropenia system is introduced with time-dependent proliferation coefficient[8,9].

Delay factors influence can't be omitted in the hematopoietic stem cell(HSCs) model due to time necessary in cell maturation[3]. As for neutrophils or granulocyte cells, Haurie analyzed the analytical form used for the density of the maturation time in bone marrow. He sums up delay factor as the total period of time that neutrophils spent in marrow and the maturation time in the blood[5,6]. He also further suggests that mechanism of CN oscillation is due to destabilization of the HSC regulation would explain the fact that the other cell lineages oscillate with the same period as the neutrophils. Bernard modelled CN in the grey collie and verified that increasing rate of apoptosis in neutrophil precursors induced the oscillation [10,11,12].

The important role of granulocyte colony-stimulating factor(G-CSF) for the in vivo control of granulopoiesis was demonstrated by Lieschke et al[13]. They showed that mice lacking G-CSF have pronounced neutropenia. G-CSF administration is routinely used to treat chronic neutropenia. Destabilization of an early HSC population resulting in oscillations with a large range of periods in all the blood elements after chemotherapy observed in CN. In Mackey's work, modification of any of the parameters in his model described can potentially induce the onset of oscillations[10,12]. Lei functioned the effect by G-CSF administration by

adding a new parameter as apoptosis rate of granulopoiesis in the blood with the consideration of maturation time[8]. To coincide with Hauire's point of view, time delay adds the period of time that neutrophils spent in marrow and the maturation time in the blood[8,9].

However, the control of granulopoiesis via the circulating neutrophil level is obscure. In this paper, we develop the discussion of peripheral neutrophil oscillation with G-CSF administration. The apoptosis rate of granulopoiesis in the blood is combined into the proliferation coefficient with point of view that elevating granulopoiesis in the marrow decreasing the circulating neutrophil number. Due to the complexity of Hopf bifurcation, the simplified quasi-static hematopoiesis system and neutropenia system are respectively discussed. The geometrical criterion developed for delay differential equations is applied in Hopf bifurcation analyzing since delay factors are also physical parameters in system. Finally, complex dynamical behaviors of the whole system are simulated numerically by the estimated apoptosis rate of neutrophil population in the blood via tracking Hopf bifurcation position in parameter space.

## 2. The mathematical model

Stem cells differentiate into more mature blood cells, including platelets, granulocytes and lymphocytes. During the process of the transition of HSCs from quiescence to cell proliferation, a clear link between the stem cell compartment and the differentiated mature cell lineages form a fully hematopoietic system which supported by tissue coupling. Quiescent phase HSCs can enter into its proliferative phase with the assumption of undergoing mitosis during time  $\tau_s$ . As a common point of view[8,10,12], a generic model which is formed corporately by hematopoietic stem cell compartment as well as neutrophil compartment can be described as the following

$$\begin{aligned} \frac{dQ}{dt} &= -(\beta(Q) + k_N(N) + k_\delta)Q + A_Q(t)\beta(Q_{\tau_s})Q_{\tau_s}, \\ \frac{dN}{dt} &= -\gamma_N N + A_N(t)k_N(N)Q_{\tau_N} \end{aligned} \quad (2.1)$$

The prominent character of the whole system lies in:

(1) Stem cells population  $Q$  is able to sustain itself through proliferation. After a cell division, the total duration of both proliferative phase assumed to be

time  $\tau_{NP}$  and maturation phase of neutropenia with time  $\tau_{NM}$  is experienced to release into circulation through the body. Platelets and lymphocytes are not included in the model other than to assume that the total differentiation rate into these two cell lines being a constant  $k_\delta$  (days<sup>-1</sup>).

(2) The rate at which stem cells differentiate into its given cell type is a function of the existing population of cells  $k_N(N)$ ;

(3) HSCs are classified as quiescent  $Q$  or proliferative phase cells and quiescent hematopoietic stem cells can enter into the proliferative phase at a rate  $\beta$ .

(4) The tissue numbers are coupled to each other through their interaction via their delayed common origin in a small pool of stem cells and the delay time which is necessary for the complete maturation process is typically a number of days.

In Eqs (2.1), The differentiation rate into neutrophil cells  $k_N$  as well as the proliferative rate  $\beta$  are considered as the holling function

$$k_N(N) = \frac{f_0 \theta_1^m}{\theta_1^m + N^m}, \quad \beta(Q) = \frac{k_0 \theta_2^n}{\theta_2^n + Q^n} \quad (2.2)$$

The surviving neutrophil cells are released into circulating cycle with death rate  $\gamma_N$  which is a constant.

Assume  $\tau_N = \tau_{NP} + \tau_{NM}$  hereafter. After differentiation from  $Q$ , the neutrophil precursors enter into a proliferative phase for a period of time  $\tau_{NP}$  (days) with proliferation rate  $\eta_{NP}(t)$ . After that, neutrophils experience a mature period  $\tau_{NM}$  and the apoptosis rate is given as a constant parameter  $\gamma_0$  due to the programmed death number. Therefore,  $A_N(t)$  is given by

$$A_N(t) = \exp \left[ \int_0^{\tau_{NP}} \eta_{NP}(t - \tau_N + s) ds - \int_{\tau_{NP}}^{\tau_N} \gamma_0(t - \tau_N + s) ds \right] \quad (2.3)$$

Similarly, the recycle rate  $A_Q(t)$  into quiescent phase  $Q$  is specially given by

$$A_Q(t) = 2 \exp \left[ - \int_0^{\tau_s} r_s(t - \tau_s + s) ds \right]. \quad (2.4)$$

For hematological normal individuals, the rate  $r_s, \eta_{NP}$  and  $\gamma_0$  are constants, and therefore,

$$A_Q = 2e^{-r_s \tau_s}, \quad A_N = e^{\tau_{NP} \eta_{NP} - \gamma_0 \tau_{NM}} \quad (2.5)$$

The estimated model parameters are referred[8] as shown in Table 1.

Parameter	Value	Unit
$k_0$	8.0	days <sup>-1</sup>
$f_0$	0.4	days <sup>-1</sup>
$k_\delta$	0.01	days <sup>-1</sup>
$\theta_1$	0.36	$\times 10^8$ cells/kg
$\theta_2$	0.3	$\times 10^6$ cells/kg
$r_s$	0.03—0.2	days <sup>-1</sup>
$\tau_s$	2.8	days
$\eta_{NP}$	2.542	days <sup>-1</sup>
$\gamma_N$	2.4	days <sup>-1</sup>
$\tau_{NM}$	6	days
$\tau_{NP}$	5	days
$\gamma_0$	0.27	days <sup>-1</sup>
$Q^*$	1.1	$\times 10^6$ cells/kg
$N^*$	6.3	$\times 10^8$ cells/kg

Table1: The values of parameters used in system (2.1).

As is well known, the hematological system usually demonstrates interesting observed dynamics. The dynamics of developed mathematical model which couple HSCs and CN population may demonstrate oscillations arise from Hopf bifurcation. DDE-Biftool [14,15] is the useful mathematical software to discover the critical values of stability switching phenomena. In this paper, we develop the traditional biological research method and previous modeling efforts to analyze and understand the intrinsic dynamical behaviors of Eqs(2.1).

### 3. Dynamics of hematopoietic stem cells

Biologically and mathematically, the models of hematopoietic system with description by delay differential equations have always given some

insights to understand the mainly factor to influence the occurrence of some abnormalities and even severe diseases. Firstly, we discuss the dynamics of hematopoietic stem cells number by developing its stability analysis under the assumption  $N = N^*$  (quiescent state of  $N$ ). We assume  $\delta = f_N + k_\delta$  with  $f_N = k_N(N^*)$  which implies per time, the quiescence number of HSCs differentiating into its tissue numbers. The decoupled dynamics of differentiation of the HSCs obeys

$$\frac{dQ}{dt} = -\delta Q - \beta(Q)Q + 2e^{-r_s \tau_s} \beta(Q(t - \tau_s))Q(t - \tau_s) \quad (3.1)$$

Setting  $\mu = 2e^{-r_s \tau_s} - 1$ , it is easily to calculate that, if  $\mu k_0 > \delta$ , Eqs(3.1) has a positive equilibrium solution

$$Q^* = \frac{[-\delta(-\mu k_0 + \delta)]^{1/2} \theta_2}{\delta}$$

underlying the assumption  $m = 1, n = 2$ .

Stability changes of the positive equilibrium solution always products the oscillating solutions periodically to predict dynamical illnesses of blood cells. Due to nonlinearity dynamics in system description, Hopf bifurcation occurs and periodic oscillating rhythms of HSC number appear.

Equation (3.1) is rewritten into its simplified version

$$\frac{dQ}{dt} = -T(Q)Q + 2e^{-r_s \tau_s} \beta(Q(t - \tau_s))Q(t - \tau_s) \quad (3.2)$$

with

$$T(Q) = \delta + \beta(Q).$$

Doing transformation  $Q = Q - Q^*$ , the linearized delay equation of Eq(3.2) is described as

$$\begin{aligned} \frac{dQ}{dt} = & -(T(Q^*) + \beta'(Q^*)Q^*)Q \\ & + 2e^{-r_s \tau_s} (\beta(Q^*) + \beta'(Q^*)Q^*)Q(t - \tau_s) \end{aligned} \quad (3.3)$$

where  $\beta'$  is the derivative of  $\beta$ .

The characteristic equation for Eq(3.3) is written as

$$\begin{aligned} \lambda + T(Q^*) + \beta'(Q^*)Q^* - (\mu + 1)(\beta(Q^*) \\ + \beta'(Q^*)Q^*)e^{-\lambda \tau_s} = 0 \end{aligned} \quad (3.4)$$

As a common point view, the occurrence of Hopf bifurcation in Eq(3.1) is due to the appearance of the imaginary roots of Eq(3.4) with zero real parts. We

set  $\lambda = i\omega$  and assume  $K = \omega\tau_s$ , then get the formula

$$\tan(K) = -\frac{\omega}{T(Q^*) + \beta'(Q^*)Q^*}, \quad (3.5)$$

$$\cos(K) = \frac{T(Q^*) + \beta'(Q^*)Q^*}{\mu\beta(Q^*) + \mu\beta'(Q^*)Q^* + \beta + \beta'(Q^*)Q^*}$$

Equation (3.5) contains  $\omega$ . If a pair of values  $(K^*, \mu)$  satisfies Eq(3.5), the single value  $\omega$  is determined as

$$\omega = -(T(Q^*) + \beta'(Q^*)Q^*) \tan(K) \quad (3.6)$$

and the corresponding  $\tau_s$  is computed as

$$\tau_s = -\frac{K}{\tan(K)(T(Q^*) + \beta'(Q^*)Q^*)} \quad (3.7)$$

Suppose  $I_K$  is a set of  $K^* + 2n\pi$  for any  $n \in \mathbb{N}$ , that is,  $I_K = \bigcup_{n=0}^{+\infty} K^* + 2n\pi$ . For any  $K$  in  $I_K$  and for any  $n$ , the corresponding critical value of  $\tau_s$  is denoted by  $\tau_{s(m)}$ ,  $m = 0, 1, 2, \dots, n$ , and sort them to satisfy

$$\tau_{s(0)}^* < \tau_{s(1)}^* < \dots < \tau_{s(n)}^*$$

The stability of solution  $Q^*$  may change as increasing  $\tau_s$  to cross some values of  $\tau_{s(m)}^*$  underlying the condition

$$\left. \text{sign} \left\{ \frac{d \text{Re } \lambda}{d \tau_s} \right|_{\tau_s = \tau_{s(m)}^*} \right\} \neq 0 \quad (3.8)$$

The following proposition[16] is introduced to verify formula (3.8).

**Proposition:** Suppose

$$P(\lambda, \mu, \tau_s) + Q(\lambda, \mu, \tau_s)e^{-\lambda\tau_s} = 0 \quad (3.9)$$

with

$$P(\lambda, \mu, \tau_s) = \lambda + T(Q^*) + \beta'(Q^*)Q^*,$$

$$Q(\lambda, \mu, \tau_s) = -(\mu + 1)(\beta(Q^*) + \beta'(Q^*)Q^*).$$

Furthermore, set

$$F(i\omega, \mu, \tau_s) = |P(i\omega, \mu, \tau_s)|^2 - |Q(i\omega, \mu, \tau_s)|^2 \quad (3.10)$$

then the equivalent formula of (3.8) is

$$\begin{aligned} \tilde{\delta}(K^*) &= \text{sign} \left\{ \frac{d \text{Re } \lambda}{d \tau_s} \right|_{\lambda = i\omega(K^*)} \right\} \\ &= \text{sign} \left\{ \frac{1}{\omega'(K^*)} \right\} \text{sign} \{ \mu'(K^*) \} \\ &\quad \text{sign} \left\{ -\frac{\omega(K^*)F_\mu}{2} \left| P(i\omega(K^*), \mu, \tau_s) \right|^2 \right. \\ &\quad \left. + [Q_{R_\mu} P_{R_{\tau_s}} - P_{R_\mu} Q_{R_{\tau_s}}] [-P_I Q_R] \right\} \end{aligned} \quad (3.11)$$

where  $Q_R, Q_I, P_R, P_I$  are the real part and imaginary part of function  $P$  and  $Q$ .

Notice that  $Q_{R_\mu} P_{R_{\tau_s}} - P_{R_\mu} Q_{R_{\tau_s}} = 0$ , Eq.(3.11) is simplified as

$$\tilde{\delta}(K^*) = \text{sign} \left\{ \frac{1}{\omega'(K^*)} \right\} \text{sign} \{ \mu'(K^*) \} \text{sign} \{ F_\mu \} \quad (3.12)$$

We further give the illustration in geometry to determine the above conditions and sign of  $\tilde{\delta}(K^*)$

with the limitation  $K^* \in I_K$ .

Firstly, From Eqs (3.5), we solve variables  $\mu, \tau$  respectively. Either of which has two branches to be described as

$$\mu_{1,2} = \frac{1}{2k_0(1 + \cos K)} (\alpha \pm \sqrt{h_0 \cos^2 K + h_1 \cos K + h_2}) \quad (3.13)$$

where

$$\alpha = (2k_\delta + 2f_N - k_0) \cos K + k_0,$$

$$h_0 = 4k_\delta^2 + 8k_\delta f_N + 4k_\delta k_0 + 4f_N^2 + 4f_N k_0 + k_0^2,$$

$$h_1 = 4k_\delta k_0 + 4f_N k_0 - 2k_0^2,$$

$$h_2 = k_0^2 - 8k_0 k_\delta - 8k_0 f_N.$$

and

$$\tau_{s1,2} = -\frac{K}{\tan K} \frac{k_0 \mu_{1,2}^2}{(f_N + k_\delta)(2f_N - \mu_{1,2} k_0 + 2k_\delta + k_0 \mu_{1,2}^2)} \quad (3.14)$$

We obtain the symmetry curve of  $\mu = \mu_{1,2}$  with respect to variable  $K \in (2n\pi, (2n+2)\pi), (n \in \mathbb{N})$ , as shown in Figure 1(a). The derivative of function  $\mu_{1,2}$  with respect to the variable  $K$  are illustrated in

Fig.1(b), which is further illustrated in details as following

For any  $k$ ,

$$\mu'(K) \begin{cases} > 0, \mu = \mu_1(K), & K \in (2k\pi, (2k+1)\pi); \\ < 0, \mu = \mu_1(K), & K \in ((2k+1)\pi, (2k+2)\pi); \\ < 0, \mu = \mu_2(K), & K \in (2k\pi, (2k+1)\pi); \\ > 0, \mu = \mu_2(K), & K \in ((2k+1)\pi, (2k+2)\pi); \end{cases} \quad (3.15)$$

We also obtain function  $\omega$  as the formula

$$\omega_{1,2} = -\frac{c \tan(K)}{k_0 u_{1,2}^2} \quad (3.16)$$

with

$$c = (f_N + k_\delta)(2f_N + 2k_\delta + k_0 u_{1,2}^2 - u_{1,2} k_0).$$

The maximum of  $\omega_1$  of  $K$  at  $K = K^{\max}$  and the decreasing of  $\omega_2$  is described in Figure2. The list of varying of derivative is

$$\omega'(K) \begin{cases} > 0, & K \in I_1, \\ < 0, & K \in I_2, \\ < 0, & K \in I_3, \\ > 0, & K \in I_4, \end{cases} \text{ and } \omega'_2(K) \begin{cases} < 0, & K \in I_5, \\ < 0, & K \in I_6. \end{cases} \quad (3.17)$$

with the assumption

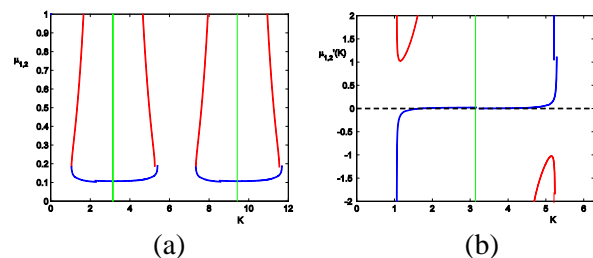


Figure 1. The function  $\mu$  of  $K$  has two branches by varying  $K$  in the interval  $(2k\pi, (2k+2)\pi)$ , here  $k = 0, 1$ . (a) the curve of  $\mu(K)$ .  $\mu_{1,2}$  are drawn respectively in red color lines and in blue color lines; (b) The derivative curves of  $\mu'_{1,2}(K)$  with  $K \in (0, 2\pi)$ .

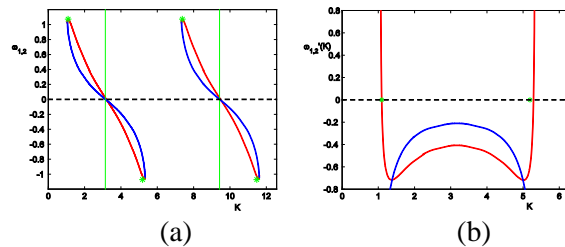


Figure 2. The function  $\omega$  of  $K$ . (a) the red curve  $\omega_1$  and the blue curve  $\omega_2$  attain its maximum at  $K^{\max} + 2k\pi$  or its minimum at  $(2k+2)\pi - K^{\max}$  with  $k = 0, 1$ . (b) the derivative of  $\omega$  w.r.  $K$  with  $K$  varying in  $(0, 2\pi)$ ,  $\omega'_1(K) = 0$  at  $K = K^{\max}$  or  $K = 2\pi - K^{\max}$  (green points).

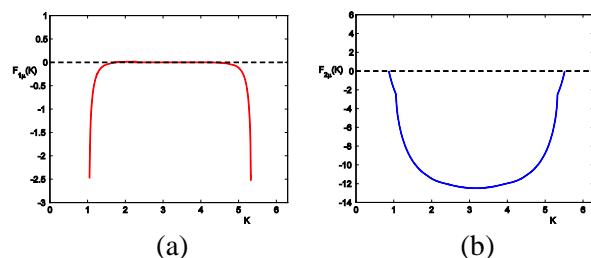


Figure 3. The derivative of  $F$  in Eq.(2.11) w.r.  $\mu$ ,  $K \in (0, 2\pi)$ , (a) the case  $\omega = \omega_1(K)$ ,  $\tau_s = \tau_{s1}(K)$ ,  $\mu = \mu_1(K)$ ; (b) another case  $\omega = \omega_2(K)$ ,  $\tau_s = \tau_{s2}(K)$ ,  $\mu = \mu_2(K)$ .

$$\begin{aligned} I_1 &= (2k\pi, K^{\max} + 2k\pi), \\ I_2 &= (K^{\max} + 2k\pi, (2k+1)\pi), \\ I_3 &= ((2k+1)\pi, (2k+2)\pi - K^{\max}), \\ I_4 &= ((2k+2)\pi - K^{\max}, (2k+2)\pi), \\ I_5 &= (2k\pi, (2k+1)\pi), \\ I_6 &= ((2k+1)\pi, (2k+2)\pi). \end{aligned}$$

and

$$F_{1\mu}(K) < 0, \quad F_{2\mu}(K) < 0. \quad (3.18)$$

By Eqs(3.13)-Eqs(3.18), the sign of  $\tilde{\delta}(K^*)$  in Eq.(3.12) is determined.

$$\tilde{\delta}(K^*) \begin{cases} > 0 & \text{when } \mu = \mu_1(K^*), K \in I_1, \\ < 0 & \text{when } \mu = \mu_1(K^*), K \in I_2, \\ > 0 & \text{when } \mu = \mu_1(K^*), K \in I_3, \\ < 0 & \text{when } \mu = \mu_1(K^*), K \in I_4, \\ > 0 & \text{when } \mu = \mu_2(K^*), K \in I_5, \\ < 0 & \text{when } \mu = \mu_2(K^*), K \in I_6. \end{cases}$$

By dynamic theory of DDEs, Hopf bifurcation occurs at points  $(\tau_{1s}(K^*), \mu_1(K^*))$  or  $(\tau_{2s}(K^*), \mu_2(K^*))$ .

The Hopf bifurcation curves are further drawn in Figure4(a). Notice to keep  $\tau_s$  positive, the discussion is underlying the assumption of parameter value of  $K$  with limitation  $2k\pi < K < (2k+1)\pi$  for any  $k$ . The whole plane is partitioned into four regimes, with  $N$ -regime below fold line denotes none existence of positive equilibrium solution. The solely positive equilibrium  $Q^*$  is stable in  $I$ -regime; However, due to Hopf bifurcation analyzed above, it changes to being unstable state which leads to periodic orbit in  $II$ -regime and  $III$ -regime. The similar discussion with logistic population model for DDEs have been reported[16,17].

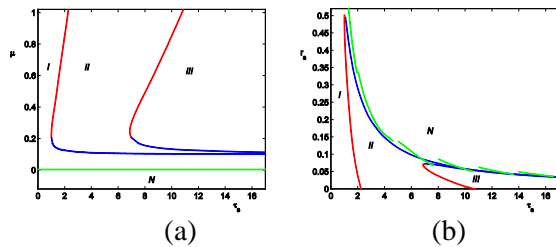


Figure 4. The curves of Hopf bifurcation with respect to Eq.(3.1). (a) Hopf bifurcation curves in  $\tau_s - \mu$  plane; (b) Hopf bifurcation curves in  $r_s - \tau_s$  plane.

#### 4. Neutrophil compartment dynamics

Hematopoiesis is a homeostatic system, consequently, most disorders of its regulation may lead to periodic dynamical diseases which exhibit transient or chronic failures in the production of one or more blood cell type. For example, one or more cellular elements of the blood are characterized by predictable oscillations. In cyclical neutropenia(CN), neutrophil

numbers oscillate and may reach a dangerous low level during its period about 19-21 days in humans and 11-16 days in dogs. Subsequently, we analyze the local dynamical behavior of the neutrophil compartment model by some theory analyzing method as well as mathematical numerical simulations.

By assuming HSCs numbers as a constant  $Q(t) = Q^*$ , we then obtain the single version dynamics for the neutrophil compartment which is modeling as

$$\frac{dN}{dt} = -\gamma_N N + A_N k_N(N(t - \tau_N))Q^* \quad (4.1)$$

where

$$k_N(N(t - \tau_N)) = \frac{f_0 \theta_1^m}{\theta_1^m + N(t - \tau_N)^m}$$

and  $A_N = e^{\eta_{NP}\tau_{NP} - \gamma_0\tau_{NM}}$ .

It is seen that Eq(4.1) balances the net production and the loss rates of circulating neutrophils in Eq.(4.1) and the measured population takes into account delay factor  $\tau_N$ , which is assumed as  $\tau_N = \tau_{NP} + \tau_{NM}$ .

As the description in Section 1, delay  $\tau_N$  physically and meaningfully expresses the total duration of the proliferative and maturation phases of the differentiated neutrophils.

By computation, the governor dynamical equation (4.1) is proved to have a positive equilibrium solution  $N^*$  with the formula

$$N^* = \frac{-\gamma_N \theta_1 + \sqrt{\gamma_N^2 \theta_1^2 + 4\gamma_N A_N f_0 \theta_1 Q^*}}{2\gamma_N}$$

Define new variable  $y(t) = N(t) - N^*$ , then the linear delay equation is expressed as

$$\frac{dy}{dt} = -\gamma_N y + B y_{\tau_N}, \quad (4.2)$$

with the coefficient  $B = A_N Q^* K'_N(N^*)$ . Therefore, the related characteristic equation is derived and written as

$$h(\lambda) = \lambda + \gamma_N - B e^{-\lambda \tau_N} = 0 \quad (4.3)$$

We assume characteristic equation (4.3) has a pair of imaginary roots, then substitute  $\lambda = i\omega (\omega > 0)$  into

$h(\lambda)$  and separate the real part from the imaginary part to get

$$\begin{aligned}\omega + B \sin(\omega \tau_N) &= 0, \\ \gamma_N - B \cos(\omega \tau_N) &= 0\end{aligned}\quad (4.4)$$

Set  $v = \omega \tau_N$  and  $Y = -B \tau_N$ , then express Eqs(4.4) as

$$\begin{cases} \tau_N = -\frac{v}{\gamma_N \tan(v)}, \\ Y = \frac{v}{\sin(v)}, \end{cases}\quad (4.5)$$

By definition of  $B$ , it satisfies that  $B < 0$ . In Eqs (4.5), therefore,  $\sin(v) > 0, \cos(v) < 0$  is

satisfied and this leads to  $v \in (\frac{\pi}{2} + 2k\pi, \pi + 2k\pi)$

for  $k = 0, 1, 2, \dots$ .

To track the Hopf bifurcation position with respect to delay  $\tau_N$ , the geometrical criterion combined with proposition 3.1 is applied.

Project an appointed value  $Y^* = -B^* \tau_N^*$ ,

furthermore, design a new function:  $(\frac{\pi}{2}, \pi) \rightarrow R$ ,

by the following definition

$$S_k(v) = \frac{v + 2k\pi}{\sin(v)}, \quad k = 0, 1, 2, \dots \quad (4.6)$$

It is observed that for any  $k \in N_0$ , if  $S_k(v^*) = Y^*$ , the characteristic equation (4.3) will have a pair of imaginary roots  $\pm i\omega(v^*)$  which lie at the value of  $(Y^*, \tau_N^*)$ . As shown in Figure5(a).

The transversal condition

$$\delta(v^*) = \text{sign} \left. \frac{d \text{Re } \lambda}{d \tau_N} \right|_{\lambda=i\omega(v^*)} \quad (4.7)$$

is determined by Eq (4.3)-Eq(4.6). The pair of imaginary roots  $\pm i\omega(v^*)$  cross imaginary axis from left to right while increasing delay  $\tau_N$ , if it meets positive  $\delta(v^*)$ ; whilst from right to left as  $\tau_N$  increasing across  $\tau_N^*$  if it meets negative  $\delta(v^*)$ .

We prove that all above discussion can be contributed to the following conclusion.

**Conclusion** For any  $k \in N_0$ , if  $S_k(V^*) = Y^*$  the characteristic equation have a pair of imaginary roots  $\pm i\omega$  at delay  $\tau_N = \tau_{N_k}$  and  $\omega \tau_{N_k} = v^*$ , as shown in Fig.5(a). and it is satisfied  $\left\{ \frac{d \text{Re } \lambda}{d \tau_N} \right\}_{\lambda=i\omega} < 0$ . Therefore, Hopf bifurcation occurs at critical values  $\tau_N = \tau_{N_k}$  for  $k = 0, 1, 2, \dots$ .

*Proof:* Set line  $L: Y^* = -B^* \tau_N^*$ .

Since

$$\frac{1}{k'_N(N)} = -\frac{\tau_N Q_* A_N}{Y}$$

it is calculated that

$$A_N = -\frac{\cos(v) \gamma_N \theta_1}{f_0 Q_* (\cos(v) + 1)^2} \quad (4.8)$$

and

$$\gamma_0 = -\frac{-\eta_{NP} \tau_{NP} + \ln \frac{-\gamma_N \theta_1 \cos(v)}{f_0 Q_* (1 + \cos(v))^2}}{\tau_{NM}} \quad (4.9)$$

With respect to the critical value  $\tau_N$ , suppose characteristic roots of Eq(4.6) can be expressed as  $\lambda(\tau_N) = \alpha(\tau_N) \pm i\beta(\tau_N)$ . and  $\lambda(\tau_N)$  satisfy  $\alpha(\tau_{N_i}) = 0, \beta(\tau_{N_i}) = \omega$  with  $\omega = \omega(v^*)$ . By substituting  $A_N, \gamma_0$  into the expression of  $B$ , with  $A_N$  and  $\gamma_0$  are respectively expressed by Eq(4.8) and by Eq(4.9). Further computation proves that

$$\begin{aligned}\delta(v^*) &= \text{sign} \left\{ \frac{d \text{Re } \lambda}{d \tau} \right\}_{\lambda=i\omega(v^*)} \\ &= \text{sign} \{ \omega'(v^*) \} \cdot \text{sign} \{ \gamma'_0(v^*) \} \cdot \text{sign} \{ BB'_{\gamma_0} \}.\end{aligned}$$

Since  $B < 0$ , we have  $\text{sign} \{ \omega'(v^*) \} < 0$  and

$\gamma'_0(v^*) \cdot B'_{\gamma_0} = B'(v^*)$ . Therefore,

$$\delta(v^*) = \text{sign} \{ BB'(v^*) \} = -\gamma_N \sec(v^*) \tan(v^*) < 0.$$

The phenomena of periodical oscillations may appear as delay  $\tau_N$  decreases to pass through corresponding Hopf bifurcation points. This makes system complex dynamical behaviors such as chaos possible. Follow-

ing we show the bounded property of parameter  $\gamma_0$  as Hopf bifurcation occurs.

#### 4.1 $\lim_{k \rightarrow \infty} \gamma_0(\tau_N)$ is bounded

*Proposition:* By Equation (4.9), as shown in Fig.5(b), Hopf bifurcation occurs on the curve line  $\gamma_0 = \gamma_0(\tau_N)$ , Now, we prove  $\lim_{k \rightarrow \infty} \gamma_0(\tau_N)$  is bounded for given  $\tau_N$ .

*Proof:* By computation,

$$Y = -B\tau_N = -e^{\eta_{NP}\tau_{NP} - \gamma_0\tau_{NM}} K'(N)Q_*\tau_N \quad (4.10)$$

Therefore,

$$e^{\eta_{NP}\tau_{NP} - \gamma_0\tau_{NM}} = \frac{Y\gamma_N^2\theta_1\tau_N}{Q_*(Yf_0 - \tau_N\gamma_N)^2} > \frac{\gamma_N^2\theta_1\frac{Y}{\tau_N}}{Q_*f_0^2\frac{Y^2}{\tau_N}}$$

which brings

$$\gamma_0\tau_{NM} < \eta_{NP}\tau_{NP} + \ln\frac{Y}{\tau_N} - \ln(\gamma_N^2\theta_1) + \ln(Q_*f_0^2) \quad (4.11)$$

Since

$$\tau_N = -\gamma_N \frac{v}{\tan(v)}$$

For given  $\tau_N$ , it is seen, there exists  $\varepsilon > 0$  which satisfy  $\varepsilon < \sin(v) < 1$  and  $-1 < \cos(v) < -\varepsilon$ .

Therefore,

$$\ln\frac{Y}{\tau_N} = \ln\left(-\frac{\gamma_N}{\cos(v)}\right)$$

$Y$  is bounded,  $\gamma_0$  is bounded to have been proven.

For fixed parameter  $\gamma_0$ , the equilibrium solution is stable if  $\tau_N$  is big enough. Varying parameter  $\gamma_0$  and  $\tau_N$ , the Hopf bifurcation curves are drawn on  $(\gamma_0, \tau_N)$  parameter space, as shown in Fig.5(b). The bifurcation curve lines are denoted as  $\gamma_0 = \gamma_0(\tau_N)$ ,  $k = 0, 1, 2, \dots$ , and it is proven that  $\lim_{k \rightarrow \infty} \gamma_0(\tau_N)$  is bounded for given  $\tau_N$ . As shown in Fig.5(b), the dense Hopf curve lines are clustered with  $k = 0, 1, \dots, 300$  and the phenomena is seldom.

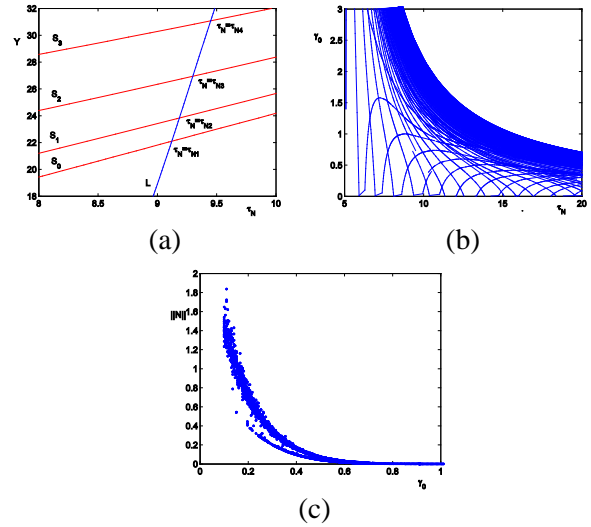


Figure5 Hopf bifurcation for linearized equation of Eq.(4.1) and multi-stability occurrence. (a) Hopf bifurcations occur at  $\tau_N = \tau_{N_k}$  for  $k = 0, 1, 2, 3$ ; (b) Hopf bifurcation curves  $\gamma_0(\tau_N)$  on  $(\tau_N, \gamma_0)$  parameter space,  $k = 0, 1, \dots, 300$ . (c) Fixed  $\tau_N = 16$ ,  $\|N\|$  denotes the difference between the maximal and the minimal values of  $N(t)$ . The solution evolution with time length 1800 days and the last 400 days are chosen.

Fixed delay  $\tau_N = 16$ , the branches amplitude  $N$  versus parameter  $\gamma_0$  is shown in Fig. 5(c). The initial values are randomly chosen, results of the distribution of  $\|N\|$  with respect to varying parameter  $\gamma_0$  further reveals the existence of different periodical solutions simultaneously.

## 5 The whole system

The whole dynamical system as the stem cell population coupling with the neutrophils is represented by Eqs(2.1). The preceding analysis for the Hopf bifurcation have predicted that the whole system may experience stability switching between stable equilibrium and unstable equilibrium. This further induces the periodic oscillation of HSCs and neutrophil numbers. The analysis of Hopf bifurcation also give us some insights to seek out the possible periodic solutions which appear at certain value of

parameters. For example, suppose  $\tau = \tau_s = \tau_N$  for simplicity, varying parameter  $r_s$ , the real part of a pair of eigenvalue changes its sign from negative to be positive, thus Hopf bifurcation occurs. By choosing

$$\tau = \tau_N = \tau_s = 14.5, \gamma_0 = 0.27, r_s = 0.02$$

we simulated periodical solution of the whole system numerically, as shown in Figure 6(a) and (b). Also chaos may happen while varying  $r_s$  due to the complexity and highly nonlinearity of system (1.1). Varying parameter  $r_s$ , the period-doubling bifurcation of periodic solutions which of system (2.1) is observed. By choosing initial values  $Q(t) = 1.6068$   $N(t) = 349.8982$   $N(t) = 349.8982$  for  $t \in [-\tau, 0]$ , the time series solution and the phase portrait for parameter  $r_s = 0.032$  is drawn in Figure 6 (c) and (d), respectively. Further choose a little bigger parameter  $r_s$ , the again period-doubling bifurcation happens. As shown in Figure 6 (e) and (f). The period-2 solution as parameter  $r_s = 0.032$  and the period-4 solution as parameter  $r_s = 0.034$  are simulated numerically.,

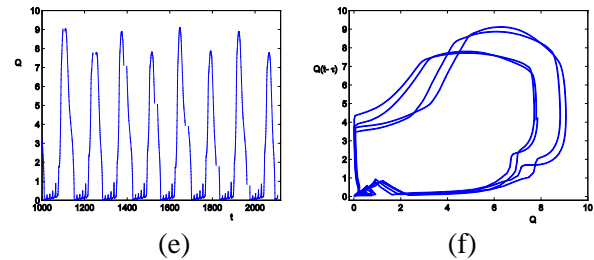
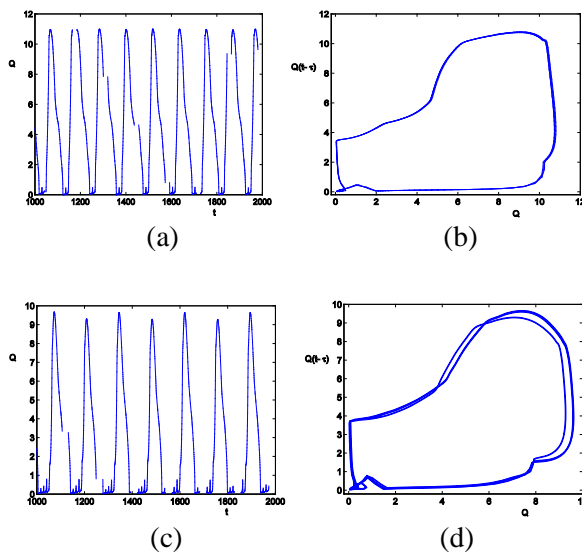


Figure 6 Periodic solution of the whole system (2.1) with different parameter  $r_s$  while choosing fixed parameters  $\tau = \tau_N = \tau_s = 14.5, \gamma_0 = 0.27$ . (a) Time series evolution solution as  $r_s = 0.02, Q$  versus  $t$ ; (b) Phase portraits of system as  $r_s = 0.02, Q(t - \tau)$  versus  $Q$ ; (c) Time series evolution solution as  $r_s = 0.032$ ; (d) Phase portraits of system as  $r_s = 0.032$  (e) Time series evolution solution as  $r_s = 0.034$  (f) Phase portraits of system as  $r_s = 0.034$ .

By choosing  $\tau_s = 16.5, \tau_N = 16$ , then varying parameters  $r_s, \gamma_0$ , the coexistence phenomena of different oscillating solutions are observed, as drawn in figure 7 and figure 8. Both regular periodic solution and unregular oscillating solution are simulated numerically as parameter values being  $\gamma_0 = 0.27, r_s = 0.032$ , as shown in Figure 7(a) and (b). Set parameter  $\gamma_0$  to be fixed, then simulation the amplitude  $N(t)$  by the difference between its maximal and its minimal values reveals the coexistence of different solutions, with parameter  $r_s$  varying in the interval  $[0.01, 0.046]$ . Choose  $\gamma_0 = 0.32, r_s = 0.016$ , the coexistence of two different periodic solutions are shown in Figure 8(a) and (b), and different solutions with oscillating rhythm are illustrated by its oscillating amplitudes of CN versus parameter  $r_s$  with  $r_s \in [0.005, 0.037]$ , as shown in Figure 8(c).

## Conclusion

All blood cells arise from a common origin in the bone marrow, the hematopoietic stem cells (HSCs). HSCs are morphologically undifferentiated cells which can either proliferate or differentiate to

produce all types of blood cells (erythrocytes, neutrophils and platelets). The development of theoretical and analytical method has given some insights in how to reveal and exhibit intrinsic dynamics of HSCs compartment. Furthermore, the findings are applied to understand the disease of cyclical neutropenia which express abnormal low level phenomena regularly. The period doubling bifurcation appears as varying apoptosis rate of HSCs in proliferation phase. The bifurcation may lead to chaotic phenomena which happen in system further. The coexistence of different oscillating rhythms of solutions via estimating Hopf bifurcation position at parameter space are observed.

### Acknowledgment

Thanks for the financial support from Chinese Natural Science Foundation.

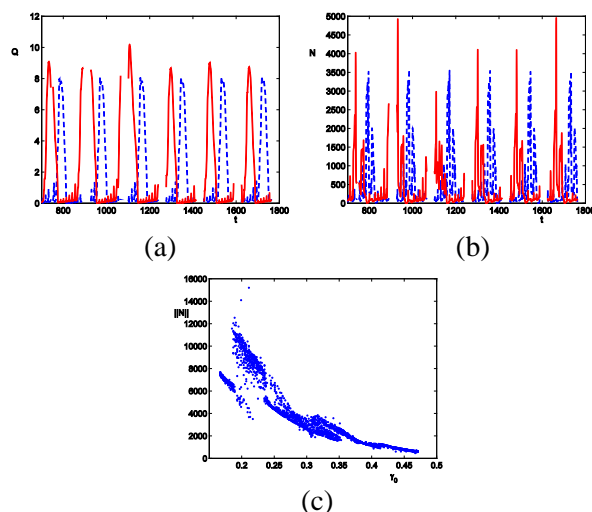


Figure 7 Different oscillating solutions coexistence in system (2.1). For  $\tau_N = 16, \tau_s = 16.5, r_s = 0.032$ . Periodic solutions with rhythms and chaos solution appear simultaneously. (a) time evolution series with  $\gamma_0 = 0.27$ ;  $Q$  versus  $t$ . (b) time evolution series with  $\gamma_0 = 0.27$ ;  $N$  versus  $t$ . (c)  $\|N\|$  denotes the difference between the maximal and the minimal values of amplitude  $N(t)$ . The solution evolution with time length 1800 days and the last 400 days are chosen.

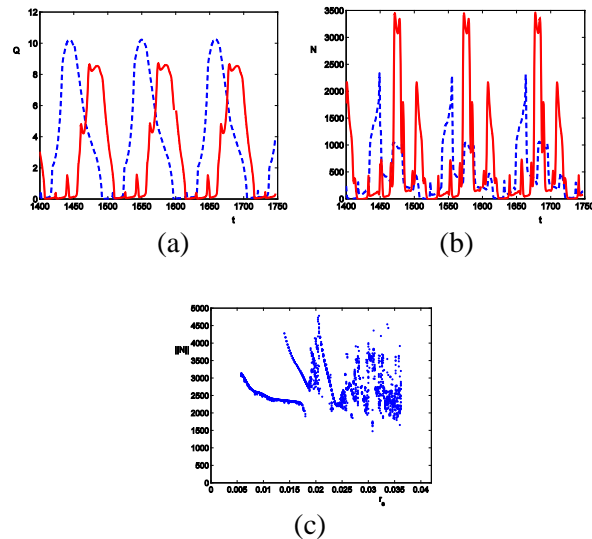


Figure 8 Different oscillating solutions coexistence in system (1.1). For  $\tau_N = 16, \tau_s = 16.5, \gamma_0 = 0.32$ , Periodic solutions with rhythms and chaos solution appear simultaneously. (a) time evolution series with  $r_s = 0.016$ ;  $Q$  versus  $t$ . (b) time evolution series with  $r_s = 0.016$ ;  $N$  versus  $t$ . (c)  $\|N\|$  denotes the difference between the maximal and the minimal values of amplitude  $N(t)$ . The solution evolution with time length 1800 days and the last 400 days are chosen.

### References

- [1] R. Apostu, M.C. Mackey, Understanding cyclical thrombocytopenia: A mathematical modeling approach. J. Theor. Biol., Vol. 251, 2008, pp, 297-316.
- [2] L.G. Israels, and E.D. Israels, Mechanisms in hematology. Core Health Services Inc, 2008.
- [3] M.C. Mackey, Mathematical models of hematopoietic cell replication and control, 1996.
- [4] M.C. Mackey, Cell kinetics status of hematopoietic stem cells. Cell prolifer., Vol. 34, 2001, pp, 71-83.
- [5] M.C. Mackey, A. A. G. Aprikyan, D.C. Dale, The rate of apoptosis in post mitotic neutrophil precursors of normal and neutropenic humans. Cell. Prolif., Vol. 36, 2003, pp. 27-34.
- [6] T. Hearn, C. Haurie and M. C. Mackey, Cyclical neutropenia and the peripheral control of white blood cell production. J. Theor. Biol., Vol. 192 1998, pp. 167-181.

- [7] C. Haurie, D.C.Dale and M. C. Mackey, Cyclical neutropenia and other periodic hematological disorders: A review of mechanisms and mathematical models. *Blood*, Vol. 92, No 8, 1998 ,pp.2629–2640.
- [8] C.J.,Zhuge, J.,Lei, and Michael C., Mackey, Neutrophil dynamics in response to chemotherapy and G-CSF, *J. Theoretical Biology*, Vol. 293 No 1,2012, pp.111-120.
- [9] J. Lei, M.C. Mackey, Multistability in an age-structured model of hematopoiesis: cyclical neutropenia., *J. Theor. Biol.*, Vol. 270, 2011, pp. 143-153.
- [10] S. Bernard, L.Pujo-Menjouet,M.C. Mackey, Analysis of cell kinetics using a cell division marker:mathematical modeling of experimental data. *J. Biophys*, Vol. 84,2003, pp.3414-3424.
- [11]S.Bernard, J. Bélair, M.C.Mackey, Oscillations in cyclical neutropenia: New evidence based on mathematical modeling, *J. heor.Biol.*, Vol. 223, 2003, pp.283-298.
- [12] C.Caroline and M. C. Mackey, Bifurcation and Bistability in a Model of Hematopoietic Regulation, *SIAM J. Applied Dynamical Systems*, Vol.6, No.2, 2007, pp. 378-394.
- [13]E. Shochat, V.Rom-Kedar, L.A. Segel, G-CSF control of neutrophil dynamics in the blood. *Bull.Math.Biol.*, Vol.69, 2007, pp. 2299-2338.
- [14]K. Engelborghs, T.Luzyanina, and D. Roose, Numerical bifurcation analysis of delay differential equations. *J. Comput. Appl. Math.*, Vol.125,2000,pp.265-275.
- [15]K.Engelborghs, T. Luzyanina, and D. Roose, Numerical bifurcation analysis of delay differential equations using DDE-BIFTOOL, *ACM Trans. Math. Software*. Vol.28, 2002, pp.1-21.
- [16] S.Q., Ma, Z.S., Feng, and Q.S., Lu, A two-parameter geometrical criteria for delay differential equations. *DCDSB*, Vol.9, No.2,2008, pp.397-413.
- [17] S.Q., Ma, Q.S., Lu and S.L. Mei, Dynamics of a logistic population model with maturation delay and nonlinear birth rate. *DCDSB*, Vol.5,No.3 2005,pp.735-752.